How to cite: *Angew. Chem. Int. Ed.* **2024**, *63*, e202401419
doi.org/10.1002/anie.202401419

Main-Group Chemistry

The Fundamental Disorder Unit in (Si, P)–(O, N) Networks

*Marwin Dialer, Kristian Witthaut, Thomas Bräuniger, Peter J. Schmidt, and Wolfgang Schnick**

Abstract: This study presents the synthesis and characterization of oxonitridosilicate phosphates $Sr_3SiP_3O_2N_7$, $Sr_5Si_2P_4ON_{12}$, and $Sr_{16}Si_9P_9O_7N_{33}$ as the first of their kind. These compounds were synthesized under high-temperature (1400 °C) and high-pressure (3 GPa) conditions. A unique structural feature is their common fundamental building unit, a *vierer* single chain of $(Si, P)(O, N)_4$ tetrahedra. All tetrahedra comprise substitutional disorder which is why we refer to it as the fundamental disorder unit (FDU). We classified four different FDU motifs, revealing systematic bonding patterns. Including literature known $Sr_5Si_2P_6N_{16}$, three of the four patterns were found in the presented compounds. Common techniques like single-crystal X-ray diffraction (SCXRD), elemental analyses, and ^{31}P nuclear magnetic resonance (NMR) spectroscopy were utilized for structural analysis. Additionally, low-cost crystallographic calculations (LCC) provided insights into the structure of $Sr_{16}Si_9P_9O_7N_{33}$ where NMR data were unavailable due to the lack of bulk samples. The optical properties of these compounds, when doped with Eu^{2+}, were investigated using photoluminescence excitation (PLE), photoluminescence (PL) measurements, and density functional theory (DFT) calculations. Factors influencing the emission properties, including thermal quenching mechanisms, were discussed. This research reveals the new class of oxonitridosilicate phosphates with unique systematic structural features that offer potential for theoretical studies of luminescence and band gap tuning in insulators.

Introduction

The learning process is significantly improved when new information is linked to existing knowledge. This approach is particularly beneficial in scientific research, where parallels are often drawn with known compounds to better understand newly discovered materials. In our case, we want to use the well-established compound class of alkaline earth and rare earth metal SiAlONs (silicon aluminum oxonitrides) to introduce the new class of alkaline earth oxonitridosilicate phosphates, or rather SiPONs. Their striking similarities serve not only as motivation to investigate such compounds in view of the diverse applications of SiAlONs, but also to facilitate the understanding of their rather complex structures.[1,2] SiAlONs are generally characterized by a tetrahedral network spanned by Al^{3+} and Si^{4+} as network-forming cations (NFC) and N^{3-} and O^{2-} as ligands. Although these networks can be neutral, we will only focus on anionic SiAlONs since the presented SiPONs include Sr^{2+} as a counter cation. The obvious difference between the two classes is that in SiAlONs the tetrahedra are occupied by Al^{3+}/Si^{4+} and in SiPONs by Si^{4+}/P^{5+} but the relationship of the pairings is the same, i.e., similar charges, ionic radii and isolobal behavior with respect to the ligands (Al–O/Si–N, Si–O/P–N). This already suggests that the nature and connectivity of the two networks should be correlated which is why we give a brief overview here. By nature, we refer to the substitutional ordering and elemental composition of the network. There are examples of all ordering types with no obvious preference for SiAlONs, e.g., $Sr_{10}Sm_6Si_{30}Al_6O_7N_{54}$ (ordered), $BaSi_5AlO_2N_7$ (partially ordered), and $Pr_4Si_5AlO_7N_7$ (disordered), but there is a strong preference for silicon-rich compositions.[3–5] In fact, we know of only one example in which Al^{3+} occupies more than 50 % of the tetrahedra, namely in $SrSiAl_2O_3N_2$.[6] This trend of mixed networks being dominated by the smaller NFC has already been mentioned in previous work.[7] The same was observed for pure nitridosilicate phosphates with $Sr_2SiP_2N_6$ (ordered), $SrSiP_3N_7$ (partially ordered), and $Sr_5Si_2P_6N_{16}$ (disordered), as well as $Sr_5Si_7P_2N_{16}$ being the only representative whose network is dominated by the larger NFC, here Si^{4+}.[7–9] The connectivity in SiAlONs known in the literature cannot easily be categorized into recurring patterns. Although most structures are composed of corner-sharing tetrahedra, their motifs range from three- to eight-membered rings, e.g., in $BaSi_5AlO_2N_7$, to distorted *vierer* single chains, e.g., in $Pr_4Si_5AlO_7N_7$, to even more complex structures.[4,5] All this could be understood as the absence of structural systematics, but the comparison of anionic SiAlONs with different counter cations can be rightly

[*] M. Dialer, K. Witthaut, Dr. T. Bräuniger, Prof. Dr. W. Schnick
Department of Chemistry
University of Munich (LMU)
Butenandtstraße 5–13, 81377 Munich (Germany)
E-mail: wolfgang.schnick@uni-muenchen.de
Dr. P. J. Schmidt
Lumileds Phosphor Center Aachen (LPCA)
Lumileds (Germany) GmbH
Philipsstraße 8, 52068 Aachen (Germany)

criticized. Especially since we will see below that Sr–(Si, P)–(O, N) compounds have a very close relationship which we refer to as the fundamental disorder unit (FDU). Given the many similarities, the question remains as to why SiPONs were not explored earlier. The answer to this is probably the more difficult synthesis, which requires high temperatures (>1400 °C) to activate the Si species, e.g., Si_3N_4 or SiO_2, and high pressures (>3 GPa) to avoid premature evaporation or decomposition of the Sr and P species, e.g., $Sr(N_3)_2$, P_3N_5 and P_4O_{10}. SiAlONs typically need significantly lower pressures (<150 MPa), which makes the synthesis easier successful outside a multianvil press. Furthermore, we have previously shown that the elucidation of the structure and in particular the network in (Si, P) compounds is a multi-step process that often utilizes high-level analytics, such as atomic-scale scanning transmission electron microscopy (STEM).[7,8] However, we are interested in making this workflow more accessible by extending the analytical scope to more common methods, such as NMR. In this contribution, we present $Sr_3SiP_3O_2N_7$, $Sr_5Si_2P_4ON_{12}$ and $Sr_{16}Si_9P_9O_7N_{33}$ as the first alkaline earth SiPONs. We analyzed their structures by a mixture of SCXRD, elemental analyses, NMR, and low-cost crystallographic calculations (LCC). To provide context and stimulate future research, we also investigated their optical properties upon doping with Eu^{2+}.

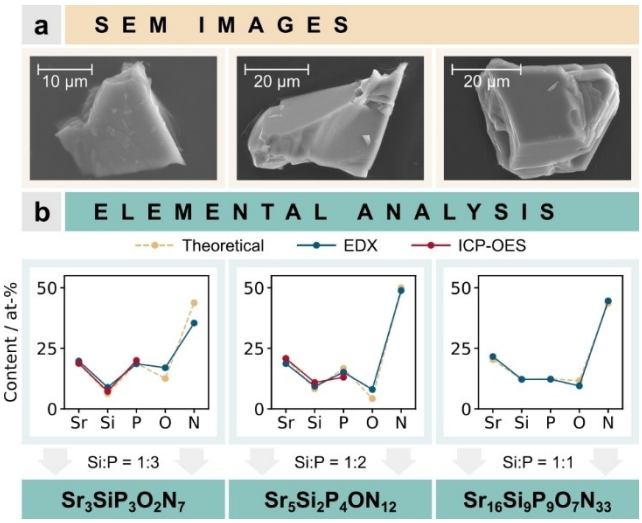

Figure 1. a) Scanning electron microscopy (SEM) images of $Sr_3SiP_3O_2N_7$, $Sr_5Si_2P_4ON_{12}$ and $Sr_{16}Si_9P_9O_7N_{33}$. b) Graphs of the EDX and ICP-OES results showing the percentage of each element on the y-axis and the respective elemental types on the x-axis.

Results and Discussion

Synthesis

Stoichiometric amounts of $Sr(N_3)_2$, SrO, amorphous Si_3N_4, amorphous SiO_2, and α-P_3N_5 were used to synthesize the compounds $Sr_3SiP_3O_2N_7$ and $Sr_5Si_2P_4ON_{12}$ according to equations 1 and 2.

$$3\ Sr(N_3)_2 + 6\ SrO + Si_3N_4 + 3\ P_3N_5 \rightarrow 3\ Sr_3SiP_3O_2N_7 + 8\ N_2 \quad (1)$$

$$30\ Sr(N_3)_2 + 3\ Si_3N_4 + 3\ SiO_2 + 8\ P_3N_5 \rightarrow 6\ Sr_5Si_2P_4ON_{12} + 80\ N_2 \quad (2)$$

After thorough mixing in an agate mortar, the starting materials were transferred to a BN crucible with a Mo inlay and heated to 1400 °C under a pressure of 3 GPa using a multianvil press. For more details on the syntheses refer to the Supporting Information. The syntheses of $Sr_3SiP_3O_2N_7$ and $Sr_5Si_2P_4ON_{12}$ resulted in colorless and microcrystalline powders with a phase fraction of the target phase higher than 90 wt % according to Rietveld refinements (Figure S1, Table S3). $Sr_{16}Si_9P_9O_7N_{33}$ appeared as a minor side phase of $Sr_5Si_2P_4ON_{12}$, while a direct synthesis was not successful.

Structure Elucidation Process

All compounds crystallize well enough to be studied by SCXRD (Figure 1a). In this way, we obtained preliminary structure models of the form $Sr_u(Si, P)_v(O, N)_w$ where u, v, and w are given by the number of sites and their multiplicities. The subdivision of the sites into Sr, (Si, P), and (O, N) sites is chemically unambiguous. This means that all atomic Sr positions can be determined solely based on X-ray diffraction due to the high X-ray contrast compared to Si, P, N and O.[10] In contrast, Si^{4+} and P^{5+} can occupy the same sites as network-forming cations with comparable charges and sizes. The same applies to the ligands N^{3-} and O^{2-}. The fundamental challenge with such networks is therefore to determine whether there is substitutional disorder of Si/P and O/N, i.e., whether a crystallographic site is occupied by more than one type of atom. The low X-ray contrast of Si/P and O/N make SCXRD an unsuitable method for this discrimination. Instead, we addressed these challenges with a complementary approach of elemental analysis, NMR spectroscopy, and LCC. In a first step, we determined the empirical sum formulas by measuring the Si:P ratio using energy-dispersive X-ray (EDX) and inductively coupled plasma optical emission spectroscopy (ICP-OES), if available (Figure 1b). The N:O ratio was extracted by enforcing charge neutrality. Considering these results and the isolobal relationship of Si–O and P–N, we obtain $Sr_3Si_{1+x}P_{3-x}O_{2+x}N_{7-x}$ ($x \approx 0.2$), $Sr_5Si_{2+x}P_{4-x}O_{1+x}N_{12-x}$ ($x \approx 0.3$–0.5), and $Sr_{16}Si_{9-x}P_{9+x}O_{7-x}N_{33+x}$ ($x \approx 0.1$). This makes them the first representatives of the oxonitridosilicate phosphates.

In the interest of readability, we will only use idealized sum formulas in this contribution where $x = 0$. In a second step, we performed solid-state NMR measurements on the bulk samples of $Sr_3SiP_3O_2N_7$ and $Sr_5Si_2P_4ON_{12}$ to investigate the substitutional ordering of the networks, while LCC provided information on the ordering of the ligands and of $Sr_{16}Si_9P_9O_7N_{33}$ as a whole, since NMR measurements were not possible on single particles. However, before we delve into the complexity of the structure elucidation process of

disordered compounds, we believe it is beneficial to first understand the final structure models and then work our way back. To do this, it is also necessary to emphasize the similarities between the three compounds $Sr_3SiP_3O_2N_7$, $Sr_5Si_2P_4ON_{12}$, and $Sr_{16}Si_9P_9O_7N_{33}$.

The Fundamental Disorder Unit

All compounds share a common fundamental building unit, which according to Liebau can be described as a *vierer* single chain of (Si, P)(O, N)$_4$ tetrahedra with a regular tetrahedral orientation of down, down, up, up (Figure 2a).[11] The tetrahedra are subject to a flexible statistical occupation of Si and P which can range from Si:P = 1:3 ($Sr_3SiP_3O_2N_7$) to Si:P = 1:2 ($Sr_5Si_2P_4ON_{12}$) to Si:P = 1:1 ($Sr_{16}Si_9P_9O_7N_{33}$). This supports the trend mentioned above that most mixed networks are dominated by the smaller NFC, here P^{5+}. In agreement with Pauling, the bridging ligands are occupied with N and the terminal ligands with O.[12–14] This structural unit is found in all disordered Sr–(Si, P)–(O, N) networks described in this work, which is why we refer to it as the fundamental disorder unit (FDU). In addition to the flexible compositions, the FDU also shows variable bonding patterns perpendicular to the chain. We illustrate this in Figure 2b for motifs of double chains, including transformations such as mirroring and translation in the chain direction. We will see below that combinations A and C are sufficient to obtain a good understanding of the title compounds. For the sake of completeness, we also consider the literature known $Sr_5Si_2P_6N_{16}$ as an example of B.[8] Combination D is yet unknown and remains the subject of future research.

Structure Description

Since our compounds crystallize in different space groups, they do not share the same reference coordinate system for the anionic (Si, P)–(O, N) networks. However, for a better comparison, we introduced a new one, in which x points in the chain direction of the FDU, y points in direction of neighboring FDUs and z points in the remaining direction perpendicular to x and y (Figure 3). The FDU motif in $Sr_3SiP_3O_2N_7$ is of type A and not connected along y. This leads to terminal ligands that are occupied by O. In z-direction, the double chains thus formed are fully condensed. As mentioned above, $Sr_5Si_2P_6N_{16}$ comprises the type B FDU motif, which is fully connected in y and z direction. This is also the reason why it is the only fully nitridic representative. It is noteworthy that although $Sr_3SiP_3O_2N_7$ and $Sr_5Si_2P_6N_{16}$ share the same Si:P ratio of 1:3, they exhibit different FDU motifs. This means that it is not the Si:P ratio that is decisive for the structure, but rather the reaction to the size of the tetrahedral gaps of the Sr–O/N lattice. In contrast, $Sr_5Si_2P_4ON_{12}$ and $Sr_{16}Si_9P_9O_7N_{33}$ differ significantly in their Si:P ratio of 1:2 and 1:1, respectively, but form quite similar FDU motifs, both of which can be assigned to type C. The difference is that the FDU motif in $Sr_5Si_2P_4ON_{12}$ is composed of two FDUs, while in $Sr_{16}Si_9P_9O_7N_{33}$ it is composed of three FDUs. These FDU motifs are not directly connected along y or z in either compound. The connection is established by a second motif, which we call the linker moiety. For better differentiation, they are marked dark green in Figure 3. The linker tetrahedra have the same mixed occupancy of the central atoms as the tetrahedra in the FDUs. The difference is that they contain terminal ligands with a substitutional disorder of N and O. The N content on these sites is 50 % for $Sr_5Si_2P_4ON_{12}$ and 12.5 % for $Sr_{16}Si_9P_9O_7N_{33}$. For more crystallographic information refer to the Supporting Information (Tables S4–S7). All crystallographic information files (CIF) are provided free of charge.[15] With this in mind, we want to take a step back and prove the substitutional disorder in our networks by NMR measurements and low-cost crystallographic calculations.

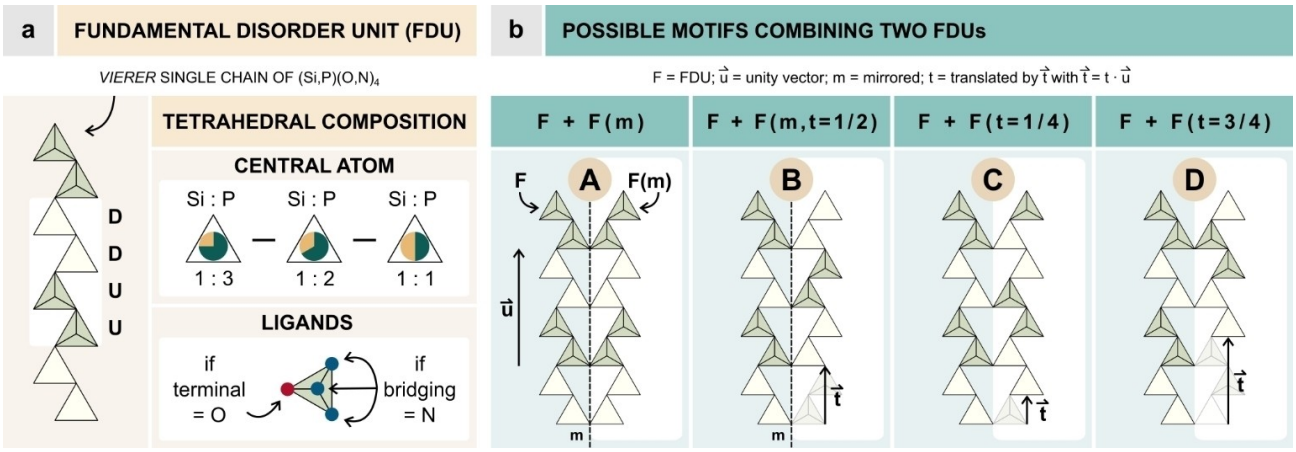

Figure 2. a) Graphical illustration of the fundamental disorder unit showing the relative orientation of the tetrahedra and the possible compositions of central atoms as well as the ligands. b) Possible FDU motifs as double chains, whereby the second motif is either mirrored (m), translated (t) or both.

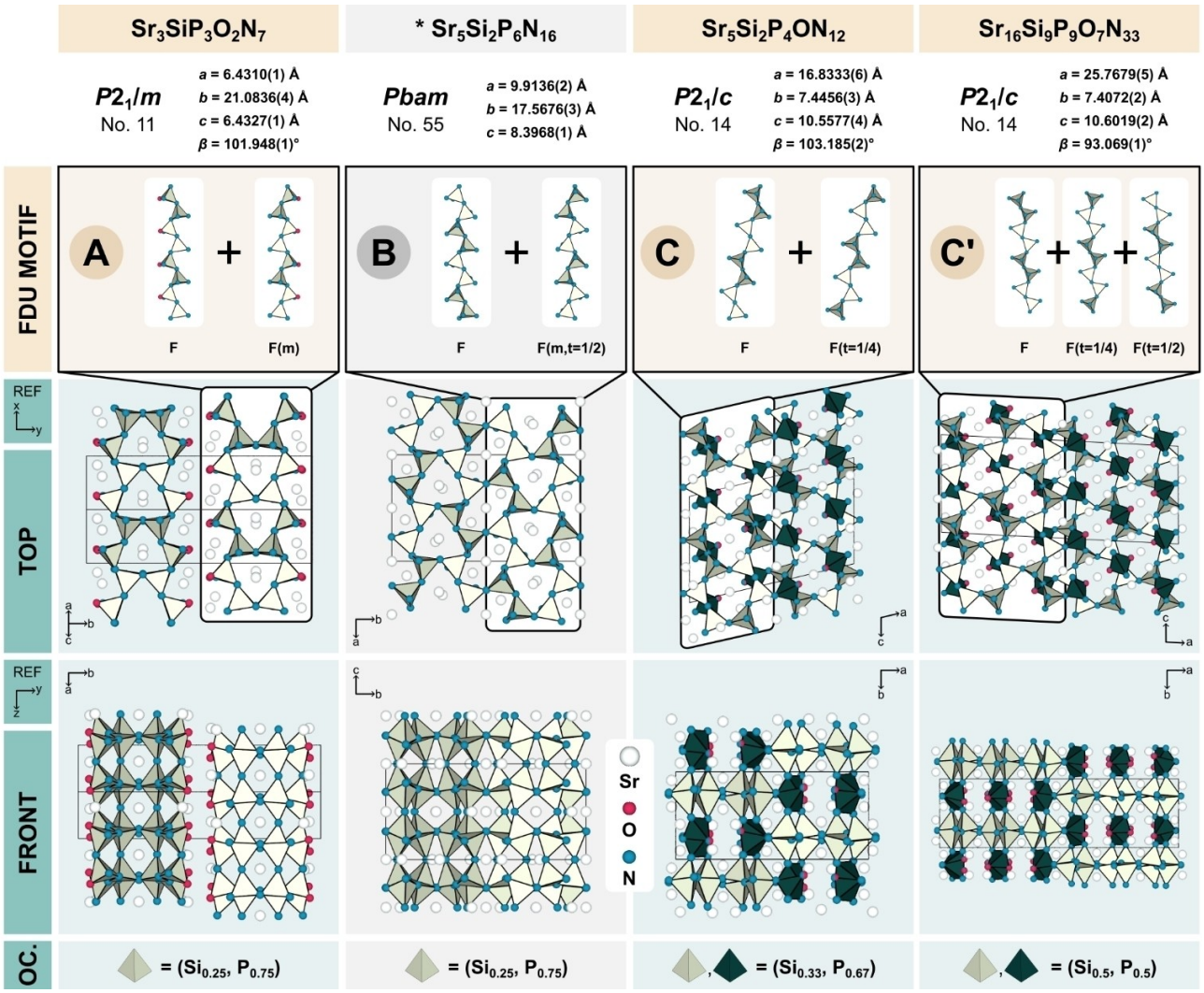

Figure 3. Crystal structures and parameters of $Sr_3SiP_3O_2N_7$, $Sr_5Si_2P_6N_{16}$ (*), $Sr_5Si_2P_4ON_{12}$, and $Sr_{16}Si_9P_9O_7N_{33}$. The FDU motifs were extracted for better visualization. Viewing directions were chosen to run along the reference coordinate system *z* (TOP) and *x* (FRONT). All tetrahedra in a compound exhibit the same occupation of central atoms. Color differentiation (light and dark green) was chosen to highlight different roles in the structure. Sr is white, N blue, and O red. (* from literature)

Nuclear Magnetic Resonance (NMR) Spectroscopy

In SiPONs, only the two spin-1/2 nuclides ^{29}Si and ^{31}P are reasonably well suited for NMR spectroscopy. The only magnetically active isotope of oxygen is ^{17}O with a very low natural abundance of about 0.4 %, which makes NMR impossible without isotope enrichment. 99.6 % of natural nitrogen consists of the nuclide ^{14}N with spin-1, which means that it has a quadrupole moment. This makes the recording and interpretation of a ^{14}N NMR signal only possible in a highly symmetric environment, which does not exist in SiPONs or SiAlONs.[16] In contrast, ^{31}P has a natural abundance of 100 %, a high Larmor frequency and acceptable relaxation times in the range of hundreds of seconds in the investigated compounds. The NMR of ^{29}Si poses a greater challenge, as the nuclide has a natural abundance of only about 5 %, a comparatively low Larmor frequency and very long relaxation times (>3000 s) in our compounds. This situation can be improved by isotopic enrichment of ^{29}Si, very long measurement times or large sample quantities. The latter two options were attempted for $Sr_3SiP_3O_2N_7$, but the resulting ^{29}Si NMR spectrum was of significantly lower quality than the ^{31}P spectra (Figure S6). Since the ^{29}Si and ^{31}P NMR results are complementary, we focused on the latter. As shown in Figure 4a for $Sr_3SiP_3O_2N_7$ and Figure 4b for $Sr_5Si_2P_4ON_{12}$, we measured ^{31}P NMR both directly and in a cross-polarized experiment with ^{1}H. The fact that the $^{31}P\{^{1}H\}$ spectra show signals should be surprising at this point, considering the hydrogen-free empirical sum formulas. However, the reason for this is a well-known phenomenon: the isolobal relationship between an oxide anion O^{2-} and an imide group $(NH)^{2-}$.

Two prominent examples of this can be found in literature with the pairings PON/P(NH)N and $Si_2ON_2/Si_2(NH)N_2$.[17–20] $(NH)^{2-}$ can also be incorporated into the structure through the isolobal relationship of Si–(NH) and

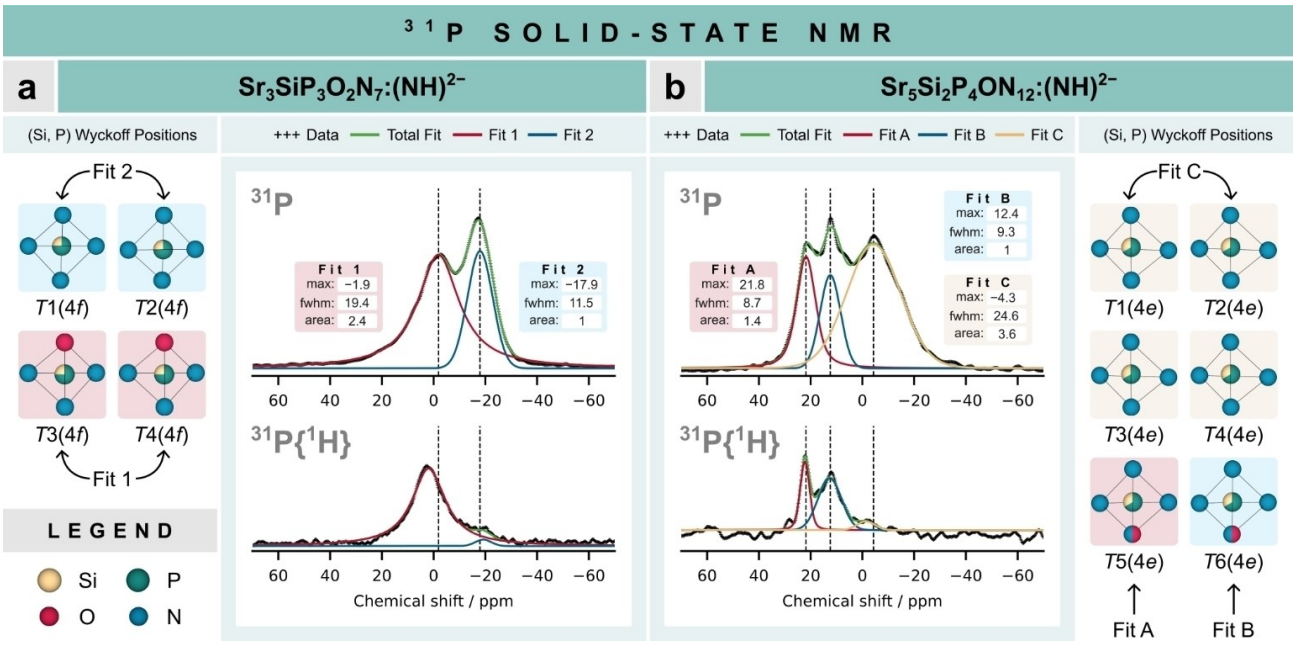

Figure 4. ^{31}P and $^{31}P\{^1H\}$ solid- state NMR spectra of (a) $Sr_3SiP_3O_2N_7:NH^{2-}$ and (b) $Sr_5Si_2P_4ON_{12}:NH^{2-}$. The curves were fitted with a combination of two or three Voigt curves. Each fit was assigned to the according Wyckoff positions, shown as red, blue, or yellow background. Their multiplicities are specified in brackets. Maxima and full widths at half-maximum (*fwhm*) are given in ppm, areas in arbitrary units. Measurements were conducted at room temperature and 20 kHz.

P–N, which becomes clear when we extend the previous example to $Si_2ON_2/Si_2(NH)N_2/SiPN_3$.[21] This raises the question of whether our empirical formulas were correct to begin with or whether H should be included. The answer is that the formulas are correct as they are. On the one hand, IR spectra of $Sr_3SiP_3O_2N_7$ and $Sr_5Si_2P_4ON_{12}$ show no significant change in transmission observed in the 3300–3600 cm^{-1} range, which is typically associated with N–H stretching vibrations (Figure S2). On the other hand, the signals of the $^{31}P\{^1H\}$ spectra are very weak, considering that the cross-polarized experiments comprised 324 scans and the direct measurements only eight. On this basis, we propose that the incorporation of $(NH)^{2-}$ is best viewed as a low-percentage doping, written as $Sr_3SiP_3O_2N_7:(NH)^{2-}$. Possible hydrogen sources are traces of hydrolysis products of SrO or SiO_2, as well as residual imide groups in amorphous Si_3N_4. The reason we devote so much space to this doping is that it was very helpful for the interpretation of our NMR spectra as we will see below. For $Sr_3SiP_3O_2N_7$, we found two broad peaks at −1.9 and −17.9 ppm with full widths at half maximum (*fwhm*) of 19.4 and 11.5 ppm, respectively (Figure 4a). This indicates two types of environments in our structure, namely (Si, P)N_4 (*T*1, *T*2) and (Si, P)ON_3 (*T*3, *T*4) tetrahedra. Which of both environments belong to which peak can be deduced from the $^{31}P\{^1H\}$ spectrum, which also shows two peaks in the same region. In our case the much stronger left peak corresponds to the (Si, P)ON_3 environment, based on the assumption that the exchange of the terminal P–O/P–(NH) is much more likely than the bridging P–N–P/P–(NH)–Si due to the chemical similarity of O^{2-} and $(NH)^{2-}$. Nevertheless, both mechanisms appear. Therefore, *T*1/*T*2 were assigned to fit 2 and *T*3/*T*4 to fit 1. For the order in the network, we argue that the widths of our signals with half-widths greater than 11 ppm are reliable indications for the mixed occupancy of the central atoms Si and P, since irregular second coordination environments, as occur in substitutional disorder, lead to a significant broadening of the signals via a chemical shift distribution. To support this argument, we have measured ^{31}P NMR of previously published $Sr_2SiP_2N_6$ and $Sr_5Si_7P_2N_{16}$, two compounds that do not exhibit Si and P mixing.[7,8] In both cases, the signals are significantly narrower with a half-width of 6.2 and 6.3 ppm, respectively (Figure S7). As for the areas of fit 1 and fit 2, we would expect a ratio of 1:1 from the Wyckoff positions, but the result is approximately 2:1 in both the ^{31}P and ^{29}Si NMR spectra (Figure S6). Since this mismatch occurs in both cases, this rules out preferential occupation of Si and P. A more reasonable explanation is the Nuclear Overhauser Effect (NOE), in which the signals from Si and P nuclei closer to ^1H nuclei may be amplified due to dipole-dipole cross-relaxation under proton decoupling.[22]

In the case of $Sr_5Si_2P_4ON_{12}$ the ^{31}P and $^{31}P\{^1H\}$ spectra show three peaks at 21.8 (fit A), 12.4 (fit B), and −4.3 ppm (fit C). Following the same principle from before, we can divide the six potential crystallographic sites of P into two groups, namely four (Si, P)N_4 environments (*T*1–*T*4) and two (Si, P)$N_3(N_{0.5}O_{0.5})$ environments (*T*5, *T*6). *T*1–*T*4 belong to the FDU motif with quite similar chemical environments, which is consistent with the very broad signal at −4.3 ppm with *fwhm* = 24.6 ppm. In contrast, *T*5 and *T*6 form the linker tetrahedra whose neighborhoods are clearly different from *T*1–*T*4. This explains why we see two additional signals with half-widths of 8.7 and 9.3 ppm for fit A and fit B, respectively. Although both signals are narrower than fit C,

they are still significantly wider than the reference signals at about 6 ppm, again indicating substitutional disorder. We propose that the upfield signal (fit B) is assigned to *T*6 due to stronger shielding, which can be inferred from the smaller tetrahedral volume ($V(T6) = 2.27$ Å^3) and smaller mean distance to O, N, and Sr ($d(T6) = 2.43$ Å) in the first and second coordination sphere compared to *T*5 ($V(T5) = 2.30$ Å^3, $d(T5) = 2.46$ Å). However, the differences are small, suggesting that theoretical chemical shift calculations are required to support this assignment. The area ratio of the fits of 1.4:1:3.6 agrees well with the theoretical ratio expected from the Wyckoff positions for $T5:T6:T1–T4 = 1:1:4$.

Although NMR is a very sensitive method that provides deep insights into our (Si, P)–(O, N) networks, there were still challenges that required complementary low-cost crystallographic calculations. One of them is the substitutional order of the ligands N and O, which has so far been taken as given without justification. Another is the overall substitutional order of both Si/P and O/N of the third compound $Sr_{16}Si_9P_9O_7N_{33}$, for which no NMR data were available due to the lack of a bulk sample.

Low-Cost Crystallographic Calculations

First, it is important to understand what kind of calculations were used and why. In previous work, we introduced "low-cost crystallographic calculations" as a generic term for widely used crystallographic concepts that require low computational resources compared to density functional theory (DFT) calculations.[7,8] In this work, we calculated (Si, P)–(O, N) bond lengths, (Si, P)(O, N)$_4$ tetrahedral volumes, as well as electrostatic potential energies (Ewald Summation), charge distributions (CHARDI), and bond valence sums (BVS) of Si^{4+} and P^{5+}.[23–28] On the one hand, we use the distributions of bond lengths and volumes in a compound to distinguish between N and O. If the distributions show a discrete clustering with a clear gap, it can be assumed in most cases that there are distinct O sites. In conjunction with Pauling's principle, according to which O^{2-} tends to occupy terminal positions, a reliable assignment of the ligands is possible.[12–14] On the other hand, the Ewald summation, CHARDI, and BVS are useful methods to evaluate the occupancy of the central atoms. However, the most important information we obtain from all methods is whether the overall atom assignment in our network is congruent. To evaluate the congruence, we need to define reference data from literature compounds for each method. In case of a pure nitridosilicate, this would be, for example, the mean Si–N bond length or the mean electrostatic potential energy of Si^{4+}. The main problem is that there is insufficient reference data for SiPONs, as Si and P need not only to be present in the reference, but also in the same ratio as in the sample. This can be remedied by calculating the corresponding expected values from pure nitridosilicates and nitridophosphates as the percentage composition as shown in equation 3 using the example of a ($Si_{0.5}$, $P_{0.5}$)–N bond length.

$$\langle d\rangle((Si_{0.5}, P_{0.5}) - N) = 0.5 \cdot \overline{d}(Si - N) + 0.5 \cdot \overline{d}(P - N) \quad (3)$$

$\langle d\rangle$: expected distance, $\overline{d}$: average distance calculated from literature

As a numerical measure of congruence, we used the total percentage deviation (D) of the sample data from these expected values. Typically, total deviations below 3 % indicate a congruent model.[7] The comparison and evaluation of all five methods for the four compounds $Sr_3SiP_3O_2N_7$ (1), $Sr_5Si_2P_6N_{16}$ (2), $Sr_5Si_2P_4ON_{12}$ (3), and $Sr_{16}Si_9P_9O_7N_{33}$ (4), are shown in Figure 5, where columns 1–5 represent each method, column 6 the total percentage deviation, rows 1–4 the respective compounds and the bottom row the reference data of pure nitridosilicates and nitridophosphates. Each cell shows a stack of all (Si, P) Wyckoff positions with their calculated values, their overall average, and their expected value. From this we can draw several conclusions: First, for compounds (1), (3) and (4), we can see that the bond lengths exhibit clustering, with the bridging ligands N comprising the longer bond lengths (blue) and the terminal ligands (O, N) the shorter bond lengths (red). The proportion of N in the terminal ligands was calculated taking charge neutrality into account and yields 0, 50, and 12.5 % for (1), (3), and (4), respectively. The clustering is also reflected in the tetrahedral volumes, however, with one exception. In $Sr_3SiP_3O_2N_7$ (1), the tetrahedral volumes of *T*1–*T*4 are approximately equal despite their different composition of (Si, P)N_4 and (Si, P)ON_3. This shows that the central atoms Si and P in this compound do not determine the structure, but only react to the Sr–O/N lattice. The bond lengths show that the central atoms move towards O as a ligand, but only at the cost of a proportional elongation of the other bonds. As a future prospect, this behavior would generally be interesting for isolobal substitutions of the counter cations and ligands, e.g., the substitution of Sr–O by La–N would yield $SrLa_2SiP_3N_9$. Second, the calculated values of the Ewald summation, CHARDI, and BVS agree very well with what we expect. This would not be the case if we assumed a wrong substitutional order of our networks, as we have shown in previous work for $Sr_5Si_2P_6N_{16}$ (2).[8] Finally, according to our definition, all networks with total deviations of 0.9–1.8 % are congruent. This completes the complex structure elucidation process of the $Sr_3SiP_3O_2N_7$, $Sr_5Si_2P_4ON_{12}$, and $Sr_{16}Si_9P_9O_7N_{33}$ compounds. Although the structural features of this new class of compounds were our main focus, we also wanted to take a closer look at their optical properties, as SiAlONs, nitridosilicates and nitridophosphates are known to exhibit excellent luminescence properties.[29,30] This was also with the ulterior motive of placing these compounds in a larger context regarding their applicability and suitability as model systems.

Optical Properties

In our research, the addition of 1 mol % Eu^{2+} to the starting materials is a standard procedure when alkaline earth metals are present. Apart from obvious reasons such as the search

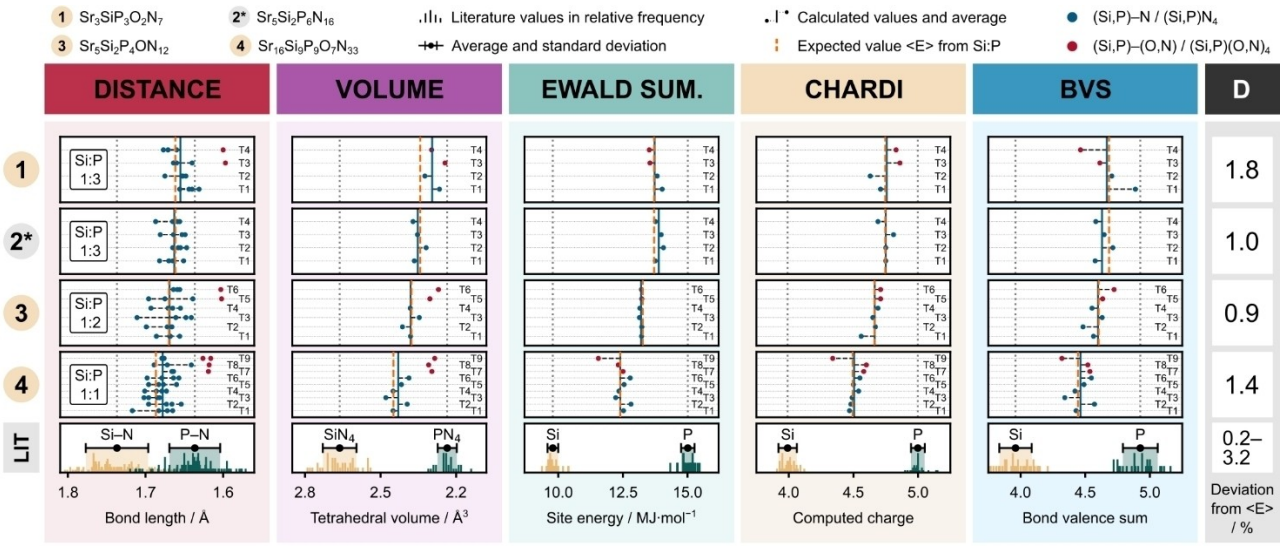

Figure 5. Graphical representation of the LCC results. Columns 1–5 show the respective methods, column 6 the total percentage deviation from expected values, rows 1–4 the compounds, and the bottom row the literature data (LIT) in relative frequency. The calculated values are marked as blue if only N is present in the first coordination sphere, otherwise red for O and N. Expected values are dashed orange lines. (Si, P)–(O, N) bond lengths and (Si, P)(O, N)$_4$ volumes were dismissed for the calculation of total deviations due to the lack of suitable reference data. (* from literature)

for new phosphor materials, this doping also serves as a useful indicator for the differentiation and separation of multiphase products. The suitability of Eu^{2+} as a dopant is not limited to its high sensitivity to its coordination environment, but also includes the fact that even low concentrations are sufficient at which no structure-altering effects normally occur. Without further analysis, the experienced eye can already gain valuable information from a purely visual inspection of the luminescence behavior of a compound. The most prominent example is the emission maxima but also the nature of the luminescence such as brightness and decay time or even absence can indicate structural features to look out for, as we will see below. In our work, we found that $Sr_3SiP_3O_2N_7$ (1) shows green emission at first glance, $Sr_5Si_2P_6N_{16}$ (2) shows orange emission, $Sr_5Si_2P_4ON_{12}$ (3) shows very weak yellow to orange emission, and $Sr_{16}Si_9P_9O_7N_{33}$ (4) shows no visible emission when irradiated with ultraviolet light. This is also reflected in the corresponding PLE and PL measurements shown in Figure 6a. Only under a luminescence microscope were we able to show that (4) also exhibits very weak orange emission. In a next step, we tried to attribute these brightness gradations to one of the following causes. First, luminescence can be quenched by N–H vibrations. As discussed above, we concluded that this is unlikely, as in this case $Sr_3SiP_3O_2N_7$ should be the most affected due to the highest amount of O/N–H. Second, we reduced the dopant concentration to less than 0.5 mol % to avoid potential concentration quenching, which resulted in no change. Third, we investigated the band gaps of all compounds to check whether photoionization as a thermal quenching mechanism is a reasonable explanation.[31] Since no bulk samples were available for (2) and (4), we decided to calculate all band gaps by periodic DFT calculations using the LMBJ functional.[32,33] This approach demonstrated to lead to band gaps that are in better agreement with experimental data than those calculated with traditional generalized gradient approximation (GGA) functionals such as PBE.[34] Nevertheless, absolute values should only give an idea about the magnitude of the gaps, while the relative differences are reliable. The resulting densities of states (DOS) were plotted in Figure 6b with the theoretical band gaps of 3.7, 3.4, 3.2, and 2.9 eV, respectively, for compounds (1)–(4). This stepwise gradation of band gaps can be interpreted as a form of band gap tuning in insulators. The main contributions to the valence band near the Fermi level come from N 2*p* and Sr 4*d* states. The same is true for the conduction band with inverse ratios. $Sr_3SiP_3O_2N_7$ is the only compound with a predicted indirect band gap, while the others are direct. All valence band minima are found at the high-symmetry Γ-point (Figures S8–S11). The decrease in band gaps agrees well with the decrease in luminescence which is why we believe that photoionization is a reasonable quenching mechanism. This could be supported by low-temperature measurements of the luminescence. However, we realize and hope that this can only be the beginning of more comprehensive studies of the electronic and optical properties of these compounds. Due to the high-pressure synthesis, their applicability is limited, nevertheless, their structural and optical relationships make them excellent model systems for theoretical calculations, such as those performed by Shafei et al. on $UCrC_4$-type phosphors.[35,36]

Conclusion

We successfully synthesized and characterized the new oxonitridosilicate phosphates $Sr_3SiP_3O_2N_7$, $Sr_5Si_2P_4ON_{12}$ and

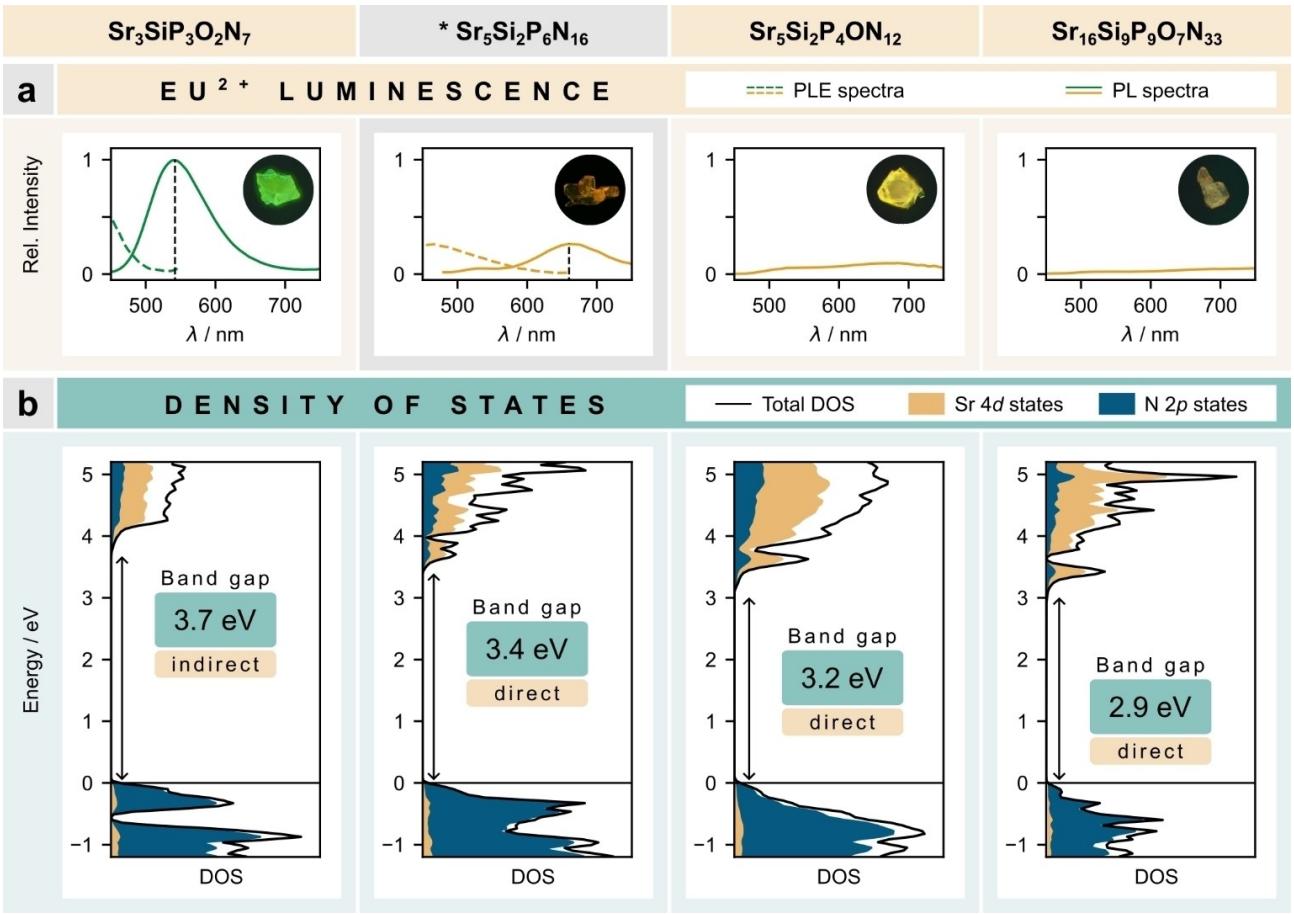

Figure 6. (a) PL and PLE spectra as well as (b) densities of states (DOS) of $Sr_3SiP_3O_2N_7$, $Sr_5Si_2P_6N_{16}$ (*), $Sr_5Si_2P_4ON_{12}$, and $Sr_{16}Si_9P_9O_7N_{33}$. Luminescence measurements were performed on single particles of comparable size at room temperature. Luminescence images were excited at 395 nm. (* PL/PLE from literature; electronic calculations original.)

$Sr_{16}Si_9P_9O_7N_{33}$, which are the first representatives of this class. The synthesis was carried out under high-temperature and high-pressure conditions and led to a phase purity of the target compounds of over 90 % for the first two, which was confirmed by Rietveld refinements. The structures of these compounds share a common fundamental disorder unit (FDU) characterized by a single *vierer* chain of (Si, P)(O, $N)_4$ tetrahedra with substitutional disorder of the central atoms. We introduced a classification of FDU motifs and showed that $Sr_3SiP_3O_2N_7$, $Sr_5Si_2P_4ON_{12}$ and $Sr_{16}Si_9P_9O_7N_{33}$, as well as $Sr_5Si_2P_6N_{16}$ known from literature, comprise three of the four possible bonding patterns. The structure elucidation process included advanced techniques such as SCXRD, EDX and ICP-OES, ^{31}P and $^{31}P\{^1H\}$ NMR, as well as low-cost crystallographic calculations. Using these methods, we were able understand the composition of the networks in which central atoms and terminal ligands exhibit substitutional disorder of Si/P and O/N, respectively. In contrast, we found that bridging ligands are only occupied by N. Compared to previous work, where we often used STEM to verify occupancy in mixed (Si, P) networks, we were able to show that ^{31}P NMR spectroscopy is a viable alternative, especially when combined with $^{31}P\{^1H\}$ NMR. In this context, we also added new ^{31}P NMR data on literature known $Sr_2SiP_2N_6$ and $Sr_5Si_7P_2N_{16}$ as reference for ordered (Si, P) networks.[7,8] LCC were used to confirm our results and provide insight into $Sr_{16}Si_9P_9O_7N_{33}$ where no NMR data were available. As an impetus for future research, we briefly investigated the optical properties of the SiPONs when doped with Eu^{2+}. To this end, we performed PLE and PL measurements as well as DFT calculations to determine the densities of states and band gaps. The differences in emission properties were attributed to various factors, including potential N–H vibrations, concentration quenching and photoionization as a thermal quenching mechanism. The latter was identified as the most likely among them. In summary, this study presents the first three representatives of oxonitridosilicate phosphates, a new class of compounds remarkable for their versatility but also for the systematic nature of the FDU motifs. The unique structure–property relationships observed in these compounds make them exciting model systems for future studies, especially in the context of luminescence and quenching mechanisms as well as band gap tuning in insulators.

Supporting Information

The authors have cited additional references within the Supporting Information.[37–63]

Acknowledgements

The authors express their gratitude to Christian Minke for providing the SEM images, EDX, and NMR measurements. Appreciation is also extended to Jennifer Steinadler for her assistance in interpreting the NMR spectra. Reinhard Pritzl and Sophia Wandelt are acknowledged for their engaging discussions and invaluable contributions to the concept and interpretation (all at Department of Chemistry, LMU Munich). M.D. also thanks the Bundesministerium für Bildung und Forschung (BMBF) for financial support. Open Access funding enabled and organized by Projekt DEAL.

Conflict of Interest

The authors declare no conflict of interest.

Data Availability Statement

The data that support the findings of this study are available in the supplementary material of this article.

Keywords: luminescence · mixed networks · DFT · oxonitridosilicate phosphates · NMR

[1] T. Yamada, T. Yamao, S. Sakata, *Key Eng. Mater.* **2007**, *352*, 173–178.
[2] R. J. Xie, *J. Ceram. Soc. Jpn.* **2020**, *128*, 710–717.
[3] R. Lauterbach, W. Schnick, *Solid State Sci.* **2000**, *2*, 463–472.
[4] S. Esmaeilzadeh, J. Grins, Z. Shen, M. Edén, M. Thiaux, *Chem. Mater.* **2004**, *16*, 2113–2120.
[5] R. Lauterbach, W. Schnick, *Z. Anorg. Allg. Chem.* **1999**, *625*, 429–434.
[6] R. Lauterbach, W. Schnick, *Z. Anorg. Allg. Chem.* **1998**, *624*, 1154–1158.
[7] M. Dialer, M. M. Pointner, P. Strobel, P. J. Schmidt, W. Schnick, *Inorg. Chem.* **2024**, *63*, 1480–1487.
[8] M. Dialer, M. M. Pointner, S. L. Wandelt, P. Strobel, P. J. Schmidt, L. Bayarjargal, B. Winkler, W. Schnick, *Adv. Opt. Mater.* **2023**, 2302668.
[9] L. Eisenburger, O. Oeckler, W. Schnick, *Chem. Eur. J.* **2021**, *27*, 4461–4465.
[10] P. J. Brown, A. G. Fox, E. N. Maslen, M. A. O'Keefe, B. T. M. Willis, in *International Tables for Crystallography Volume C: Mathematical, Physical and Chemical Tables* (Ed.: E. Prince), Springer Netherlands, Dordrecht, **2004**, p. 554.
[11] F. Liebau, *Structural Chemistry of Silicates*, Springer Berlin Heidelberg, Berlin, Heidelberg, **1985**.
[12] A. Fuertes, *Inorg. Chem.* **2006**, *45*, 9640–9642.
[13] J. George, D. Waroquiers, D. Di Stefano, G. Petretto, G. M. Rignanese, G. Hautier, *Angew. Chem. Int. Ed.* **2020**, *59*, 7569–7575.
[14] L. Pauling, *The Nature of the Chemical Bond, An Introduction to Modern Structural Chemistry*, Cornell University Press, Ithaca, **1960**.
[15] Deposition Number(s) 2325125 (for $Sr_3SiP_3O_2N_7$), 2325127 (for $Sr_5Si_2P_4ON_{12}$), 2325128 (for $Sr_{16}Si_9P_9O_7N_{33}$) contain(s) the supplementary crystallographic data for this paper. These data are provided free of charge by the joint Cambridge Crystallographic Data Centre and Fachinformationszentrum Karlsruhe Access Structures service.
[16] T. Bräuniger, P. Kempgens, R. K. Harris, A. P. Howes, K. Liddell, D. P. Thompson, *Solid State Nucl. Magn. Reson.* **2003**, *23*, 62–76.
[17] J. M. Léger, J. Haines, C. Chateau, G. Bocquillon, M. W. Schmidt, S. Hull, F. Gorelli, A. Lesauze, R. Marchand, *Phys. Chem. Miner.* **2001**, *28*, 388–398.
[18] W. Schnick, J. Lücke, *Z. Anorg. Allg. Chem.* **1992**, *610*, 121–126.
[19] C. Brosset, I. Idrestedt, *Nature* **1964**, *201*, 1211.
[20] D. Peters, H. Jacobs, *J. Less-Common Met.* **1989**, *146*, 241–249.
[21] H. P. Baldus, W. Schnick, J. Lücke, U. Wannagat, G. Bogedain, *Chem. Mater.* **1993**, *5*, 845–850.
[22] D. Neuhaus, in *Encyclopedia Magnetic Resonance*, John Wiley & Sons, Ltd, Chichester, UK, **2011**.
[23] L. Link, R. Niewa, *J. Appl. Crystallogr.* **2023**, *56*, 1855–1864.
[24] A. Y. Toukmaji, J. A. Board, *Comput. Phys. Commun.* **1996**, *95*, 73–92.
[25] M. Nespolo, *Acta Crystallogr. Sect. B* **2016**, *72*, 51–66.
[26] M. Nespolo, B. Guillot, *J. Appl. Crystallogr.* **2016**, *49*, 317–321.
[27] A. Altomare, C. Cuocci, C. Giacovazzo, A. Moliterni, R. Rizzi, N. Corriero, A. Falcicchio, *J. Appl. Crystallogr.* **2013**, *46*, 1231–1235.
[28] K. Momma, F. Izumi, *J. Appl. Crystallogr.* **2011**, *44*, 1272–1276.
[29] M. H. Fang, Z. Bao, W. T. Huang, R. S. Liu, *Chem. Rev.* **2022**, *122*, 11474–11513.
[30] S. Hariyani, M. Sójka, A. Setlur, J. Brgoch, *Nat. Rev. Mater.* **2023**, *8*, 759–775.
[31] P. Dorenbos, *J. Mater. Chem. C* **2023**, *11*, 8129–8145.
[32] T. Rauch, M. A. L. Marques, S. Botti, *J. Chem. Theory Comput.* **2020**, *16*, 2654–2660.
[33] T. Rauch, M. A. L. Marques, S. Botti, *Phys. Rev. B* **2020**, *101*, 245163.
[34] J. P. Perdew, K. Burke, M. Ernzerhof, *Phys. Rev. Lett.* **1996**, *77*, 3865–3868.
[35] R. Shafei, D. Maganas, P. J. Strobel, P. J. Schmidt, W. Schnick, F. Neese, *J. Am. Chem. Soc.* **2022**, *144*, 8038–8053.
[36] R. Shafei, P. J. Strobel, P. J. Schmidt, D. Maganas, W. Schnick, F. Neese, *Phys. Chem. Chem. Phys.* **2024**, accepted.
[37] A. Stock, H. Grüneberg, *Ber. Dtsch. Chem. Ges.* **1907**, *40*, 2573–2578.
[38] R. Suhrmann, K. Clusius, *Z. Anorg. Allg. Chem.* **1926**, *152*, 52–58.
[39] R. M. Pritzl, N. Prinz, P. Strobel, P. J. Schmidt, D. Johrendt, W. Schnick, *Chem. Eur. J.* **2023**, *29*, e202301218.
[40] D. Walker, M. A. Carpenter, C. M. Hitch, *Am. Mineral.* **1990**, *75*, 1020–1028.
[41] D. C. Rubie, *Phase Transitions* **1999**, *68*, 431–451.
[42] H. Huppertz, *Z. Kristallogr. Cryst. Mater.* **2004**, *219*, 330–338.
[43] E. Bertschler, R. Niklaus, W. Schnick, *Chem. Eur. J.* **2017**, *23*, 9592–9599.
[44] M. Mallmann, S. Wendl, P. Strobel, P. J. Schmidt, W. Schnick, *Chem. Eur. J.* **2020**, *26*, 6257–6263.
[45] A. Marchuk, L. Neudert, O. Oeckler, W. Schnick, *Eur. J. Inorg. Chem.* **2014**, *2014*, 3427–3434.
[46] SAINT, Data Integration Software, Madison, Wisconsin, USA, **1997**.
[47] Bruker-AXS, XPREP Reciprocal Space Exploration, Vers. 6.12, Karlsruhe, **2001**.

[48] Bruker-AXS, APEX4, v2021.10-0, Karlsruhe, Germany, **2021**.
[49] G. M. Sheldrick, SHELXS-97, Program of the Solution of Crystal Structure, University of Göttingen, Göttingen, **1997**.
[50] G. M. Sheldrick, *Acta Crystallogr. C Struct. Chem.* **2015**, *71*, 3–8.
[51] L. J. Farrugia, *J. Appl. Crystallogr.* **2012**, *45*, 849–854.
[52] H. M. Rietveld, *J. Appl. Crystallogr.* **1969**, *2*, 65–71.
[53] A. A. Coelho, TOPAS-Academic v4.1, **2007**.
[54] R. W. Cheary, A. A. Coelho, *J. Appl. Crystallogr.* **1992**, *25*, 109–121.
[55] R. W. Cheary, A. A. Coelho, J. P. Cline, *J. Res. Natl. Inst. Stand. Technol.* **2004**, *109*, 1.
[56] G. Kresse, J. Hafner, *Phys. Rev. B* **1993**, *47*, 558.
[57] G. Kresse, J. Hafner, *Phys. Rev. B* **1994**, *49*, 14251.
[58] G. Kresse, J. Furthmüller, *Comput. Mater. Sci.* **1996**, *6*, 15–50.
[59] G. Kresse, J. Furthmüller, *Phys. Rev. B* **1996**, *54*, 11169.
[60] G. Kresse, D. Joubert, *Phys. Rev. B* **1999**, *59*, 1758.
[61] P. E. Blöchl, *Phys. Rev. B* **1994**, *50*, 17953.
[62] H. J. Monkhorst, J. D. Pack, *Phys. Rev. B* **1976**, *13*, 5188.
[63] L. Bellaiche, D. Vanderbilt, *Phys. Rev. B* **2000**, *61*, 7877.

Manuscript received: January 20, 2024
Accepted manuscript online: February 10, 2024
Version of record online: February 26, 2024